Tricritical behavior of two-dimensional intrinsic ferromagnetic semiconducting $CrGeTe_3$

G. T. Lin[1, 2], H. L. Zhuang[3], X. Luo[1*], B. J. Liu[2,4],F. C. Chen[1,2], J. Yan[1,2],Y. Sun[2,4], J. Zhou[5], W. J. Lu[1], P. Tong[1], Z. G. Sheng[4,6], Z. Qu[4], W. H. Song[1], X. B. Zhu[1], and Y. P. Sun[4,1,6*]

[1] *Key Laboratory of Materials Physics, Institute of Solid State Physics,Chinese Academy of Sciences, Hefei, 230031, China*

[2]*University of Science and Technology of China, Hefei, 230026, China*

[3]*Department of Mechanical and Aerospace Engineering, Princeton University, Princeton, New Jersey 08544, USA*

[4] *High Magnetic Field Laboratory, Chinese Academy of Sciences, Hefei, 230031, China*

[5]*MIIT Key Laboratory of Critical Materials Technology for New Energy Conversion and Storage, School of Chemistry and Chemical Engineering, Harbin Institute of Technology, Harbin 1500001, China*

[6]*Collaborative Innovation Center of Advanced Microstructures, Nanjing University,Nanjing, 210093, China*

[*]Corresponding authors: xluo@issp.ac.cn and ypsun@issp.ac.cn.

Abstract

$CrGeTe_3$recently emerges as a new two-dimensional (2D) ferromagnetic semiconductorthat is promising for spintronic device applications. Unlike $CrSiTe_3$whose magnetism can be understood using the 2D-Ising model, $CrGeTe_3$exhibits a smaller van der Waals gap and larger cleavage energy,which could lead to a transition of magnetic mechanismfrom 2Dto 3D.To confirm this speculation, we investigate the critical behavior$CrGeTe_3$ around the second-order paramagnetic-ferromagnetic phase transition. We obtain the critical exponents estimated by several commonexperimental techniques including the modified Arrott plot, Kouvel-Fisher method and critical isotherm analysis, which showthat the magnetism of $CrGeTe_3$follows the tricritical mean-field model with the critical exponents β, γ, and δ of 0.240 ± 0.006, 1.000 ± 0.005, and5.070 ± 0.006, respectively, at the Curie temperature of 67.9 K. We therefore suggest that the magnetic phase transition from 2D to 3D for $CrGeTe_3$should locatenear a tricritical point. Our experiment providesa direct demonstration of the applicability of the tricritical mean-field model to a 2D ferromagnetic semiconductor.

Since the successful exfoliation of single layer graphene, 2D materials have been attracting significant interest due to their highly tunable physical properties and immense potential in scalable device applications [1-5]. However, pristine graphene exhibits no bandgap and its inherent inversion symmetry suppresses the spin-orbit coupling (SOC)[6-11]. The weak SOC and zero bandgapeliminate graphene as a potential candidate forbeing applied to spintronic devices,which require one to search for alternative 2D materials that extend beyond graphene to other layered materialswith van der Waals gaps [7-11]. For example, in single-layer MoS_2, the large SOC leads to a unique spin-valley coupling which may be useful for spintronic applications [12-16]. Whereas spintronic devicesusing 2D materials arestill in their infancy[17-20], which is due to the lack of long-range ferromagnetic order that is crucial for macroscopic magnetic effects[21,22].The emergence of ferromagnetism in 2D materials in combinationwith their rich electrical and optical properties could open up ample opportunities for 2D magnetic, magneto-electric, and magneto-optic applications[18,19,23].

Recently,Chromium Tellurides$CrXTe_3$ (X = Si, Ge, and Sn) with the centrosymmetric have arisen significant attention because they belong to a rare category of ferromagnetic semiconductors possessing a 2D layered structure [7,23-35]. Extensive theoretical and experiment efforts have been extended towards understanding the properties of these 2D magnets. On the theoretical side, recent studies on $CrXTe_3$ have been focusing on their electronic structure and magnetic properties, particularly predictions of the single-layer properties[24,28-33]. On the

experimental side, $CrSiTe_3$ and $CrGeTe_3$ have been prepared and characterized[7,23,25-27,34,35]. Comparing with $CrSiTe_3$, showing characteristics of a 2D-Ising behavior[7,34,35], the smaller van der Waals gap and the larger in-plane nearest-neighbor Cr-Cr distance in $CrGeTe_3$ enhance the Curie temperature from 32 K for the $CrSiTe_3$ to 61 K for the $CrGeTe_3$[7,25,28,31]. In addition, theoretical investigations have suggested that the single-layer$CrGeTe_3$ presents characteristics of 2D-Ising behavior similar to $CrSiTe_3$[31,33]. By contrast,a scanning magneto-optic Kerr microscopy experiment, single-layer$CrGeTe_3$ represents a close-to-ideal 2D Heisenberg ferromagnetic system using the rigorous renormalized spin wave theory analysis and calculations[23]. It is known that, withthe increase of the *X* atom radius, Cr*X*Te_3 presents the smaller van der Waals gap and the larger cleavage energy [7,25,28,31]. We supposethat Cr*X*Te_3 system may undergo a three dimensional (3D) magnetic phase transition from 2D with the increase of the *X* atom radius. Therefore, a method to rapidly characterize thecritical behaviorof single-crystalline $CrGeTe_3$is crucial.For this purpose, we present a detailed investigation of the critical phenomena of $CrGeTe_3$using the initial isothermal $M(H)$ curves around the Curie temperature T_C. We find that the critical exponents of $CrGeTe_3$ satisfy the universality class of the tricritical mean-field theory. This indicates that the magnetic phase transition of $CrGeTe_3$ should be close to a tricritical point from 2D to 3D.

Samples of single-crystalline $CrGeTe_3$ were prepared by the self-flux technique[26].The XRDdata indicated that the powders are singlephase with the rhombohedral structure (see Supporting Information). We measured the heat capacity

using the Quantum Design physical properties measurement system (PPMS-9T) and characterized the magnetic properties by the magnetic property measurement system (MPMS-XL5).Density functional theory (DFT) calculations were performed using Vienna *Ab-initio* Simulation Package[36]. We used the local density approximation[37,38] to treat the electron-electron exchange-correlation interactions. The electron-ion interactions are described by the potentials based on the projector augmented wave method[39,40].

Figure 1 (a) and (b) show the inverse of temperature-dependent susceptibility $1/\chi(T)$ of $CrGeTe_3$ under field cooled cooling with applied magnetic field H = 100 Oe, parallel to the *ab* plane and *c* axis, respectively. We observe a paramagnetic–ferromagnetic (PM-FM) transition that occurs at a critical temperature T_C^{mag} of 67.3 K,as determined by the derivative of the susceptibility.This temperature is consistent with the values of 61 K or 70 K reported previously[25-27]. For a FM system, the $1/\chi(T)$ above T_C^{mag} can be described by the Curie-Weiss law resulting from the mean-fieldtheory[41]. The red curves showing the Curie-Weiss law are obeyed only at high temperature. A close observation of Fig.1 (a) and (b) reveals that the $1/\chi(T)$ curves deviate from straight lines at around 150 K, which is much higher than T_C^{mag}, indicating strong short-range FM spin interactions in $CrGeTe_3$above T_C^{mag}. The effective magnetic moment is determined to be μ_{eff} ~ 4.22 μ_B (parallel the *ab* plane) and 4.35 μ_B (parallel the *c* axis), which are close to the theoretical value expected for Cr^{3+} of 3.87 μ_B [25]. The insets of Fig.1 (a) and (b)show the isothermal magnetization$M(H)$ at 5 K exhibiting a typical FM behavior with the saturation field

$H_S$of about 5 kOe (parallel to the *ab* plane) and 2.5 kOe (parallel to the *c* axis). In addition, the *M*(*H*)curves show almost no coercive force for $CrGeTe_3$.

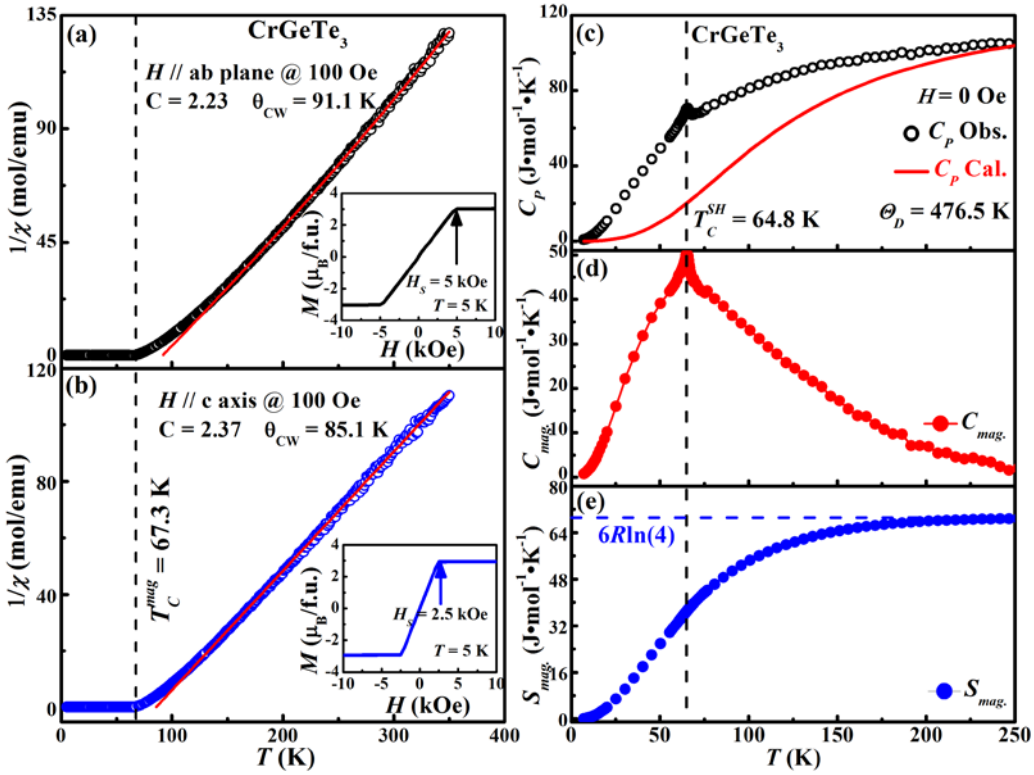

Figure 1.(Color online): (a) and (b) Inverse of temperature-dependent susceptibility $1/\chi(T)$ of $CrGeTe_3$ under field cooled cooling with an applied magnetic field *H* of 100 Oe, parallel to the *ab* plane and *c* axis, respectively. The red solid lines are the fitted results according to the Curie-Weiss law. The insets show the isothermal magnetization curves*M*(*H*) at 5 K.(c) Specific heat C_p as a function of *T* for $CrGeTe_3$ and the fitted $C_V^{\mathrm{Debye}}(T)$ using Eq. (1) and (2); Temperature-dependent magnetic (d) specific heat $C_{\mathrm{mag}}(T)$ and (e) entropy $S_{\mathrm{mag}}(T)$. The blue dashed line refers to $S_{\mathrm{mag}}(T\rightarrow\infty)$ calculated with the magnetic moment S of Cr^{3+} being 3/2.

Figure 1(c) shows the variation of the zero-field specific heat (SH)$C_p(T)$ with temperature. The sharp anomaly in $C_p(T)$ at 64.8 K corresponds to the Curie temperature $T_{\mathrm{C}}^{\mathrm{SH}}$ .Since $CrGeTe_3$ is a seminconductor[25],the electronic contribution to the heat capacity is not considered. The C_{mag}can be calculated by the following equations[41]:

$$C_{\mathrm{mag}}(T) = C_p(T) - NC_V^{\mathrm{Debye}}(T), \quad (1)$$

$$C_V^{\text{Debye}}(T) = 9R\left(\frac{T}{\Theta_D}\right)^3 \int_0^{\Theta_D/T} \frac{x^4 e^x}{\left(e^x - 1\right)^2} dx\,, \qquad (2)$$

where R is the molar gas constant, Θ_D is the Debye temperature, and N = 5 is the number of atoms per formula unit. The sum of Debye functions accounts for the lattice contribution to specific heat. We can extract the magnetic contribution $C_{\text{mag}}(T)$ from the measured specific heat of $CrGeTe_3$. The fitted $C_p(T)$ for $CrGeTe_3$ by Eq. (1)and (2) over the temperature range from about 7 to 250 K is shown by the red curve in Fig.1(c) using the Debye temperature Θ_D= 476.5 K. We observe a sharp peak at T_C^{SH} of 64.8 K and there is strong dynamic short-range FM spin interactionsabove T_C^{SH} (shown in the Fig.1(d)). The magnetic entropy $S_{\text{mag}}(T)$is calculated by $S_{\text{mag}}(T) = \int_0^T \frac{C_{\text{mag}}(T)}{T} dT$ .Fig.1 (e) shows the temperature dependence of $S_{\text{mag}}(T)$. The entropy of $CrGeTe_3$per mole with completely disordered spins S is $S_{mag}(T \to \infty) = 6R\ln(2S+1)$ .Using S = 3/2 for Cr^{3+}, we obtain $S_{\text{mag}}(T \to \infty)$ of 69.2 J/(mol·K).As shown in Fig.1(e), one observes that the 64.7 J/(mol·K) of $S_{\text{mag}}(T)$ at 150 K is close to the value of $S_{\text{mag}}(T \to \infty)$, which suggests that $CrGeTe_3$ presents the obvious PM behavior above 150 K. However, we observe the S_{mag} is 36.3 J/(mol·K) at T_C^{SH}, which is only 52.5% of the value for $S_{\text{mag}}(T \to \infty)$ in Fig.1(e). These results indicate there is strong dynamic short-range FM spin interactions between T_C^{SH} and 150 K, which is consistent with the above conclusion from fitting the $1/\chi(T)$ data to the Curie-Weiss law.

As mentioned above, with the X atom radiusincreases,the $CrXTe_3$compounds present the smaller van der Waals gap and the larger cleavage energy[7,25,28,31],

which may induce a 3D magnetic phase transition. Forthe purpose of confirmation, we performed a detailed characterization of the critical phenomena using the initial isothermal $M(H)$ curves around T_C for the $CrGeTe_3$, which are shown in Fig.2(a).

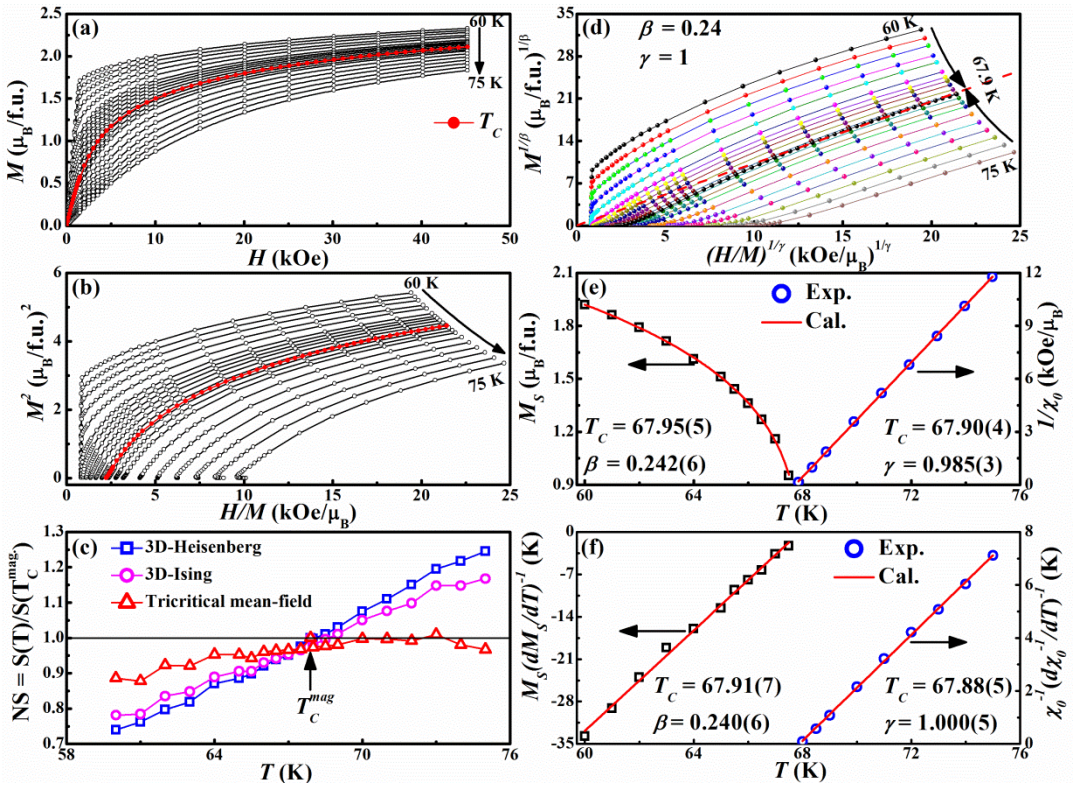

Figure 2. (Color online): (a) Initial magnetization of $CrGeTe_3$ around T_C; (b) Arrott plots of M^2 versus H/M (the $M(H)$ curves are measured at temperature intervals of 1 K and 0.5 K approaching T_C);(c) Normalized slopes as a function of temperature; (d) Modified Arrott plot ($M^{1/\beta}$versus $(H/M)^{1/\gamma}$) of isotherms withβ =0.24 and γ =1 for $CrGeTe_3$. The red dashed line is the linear fit of isotherm at 67.9 K; (e) Temperature dependence of $M_S$and χ_0^{-1}. The T_C and critical exponents are obtained from the fitting of Eq. (S1) and (S2); (f) The Kouvel-Fisher plot. The T_C and critical exponents are obtained from the linear fit.

In the mean-field theory, the critical exponents and critical temperature can be determined from the Arrott plot withβ of 0.5 and γ of 1.0[42,43]. According to this method, the M^2 versus H/M (shown in Fig.2(b)) should be a series of parallel straight lines in the higher field range around T_C and the line at $T = T_C$ shouldpass through the origin. Note that the lower field data mainly represent the arrangement of magnetic domains, which should be excluded in the fitting process[44]. However, all the curves

in Fig.2 (b) show nonlinear behaviors having downward curvature even in high field, which indicates non-mean-field-like behavior. Moreover, the positive slope reveals a second-order phase transition according to the criterion proposed by Banerjee[45]. As such, a modified Arrott plot should be employed to obtain the critical exponents.

To determine an accurate model, we obtain a modified Arrott plot following Eq. (S9) for single-crystallineCrGeTe$_3$ at different temperatures. Three groups of possible exponents belonging to the 3D Heisenberg model (β = 0.365, γ = 1.386), 3D-Ising model (β = 0.325, γ = 1.24) and tricritical mean-field model (β = 0.25, γ = 1.0) exhibit nearlystraight lines in the high field region[46,47]. We calculate their normalized slopes (NS)defined as $\mathrm{NS} = S(T) / S(T_C^{\mathrm{mag}} = 67.3\mathrm{K})$ .By comparing NS with the ideal value of unity, one can identify the most suitable model[46,47]. Figure 2(c)shows the plots of NS versus *T*employing the three different models, revealing that the tricritical mean-field model is the most appropriate to describe the critical behavior of CrGeTe$_3$.By proper selections of β and γ, one can clearly show the isotherms are a set of parallel straight lines in high fields as displayed in the Fig.2(d). The linear extrapolation from the high field region gives the spontaneous magnetization $M_S(T,0)$ and the inverse of initial susceptibility $\chi_0^{-1}(T,0)$ (seeFig.2 (e)) corresponding the interceptsonthe $M^{1/\beta}$ and $(H/M)^{1/\gamma}$axes, respectively. By fittingthe data of$M_S(T,0)$ and $\chi_0^{-1}(T,0)$to Eq. (S1) and (S2), one obtains two new values of β = 0.242 ± 0.006 with T_C = 67.95 ± 0.01 and γ = 0.985 ± 0.009 with T_C = 67.90 ± 0.09. These results are again very close to the critical exponents of tricritical mean-field model. In addition, these critical exponents and T_C can be obtained more accurately from the

Kouvel-Fisher (KF) method[48]. Hence, onecan find that the temperature dependence of $M_S(dM_S/dT)^{-1}$ and $\chi_0^{-1}(d\chi_0^{-1}/dT)^{-1}$ should be straight lines with slopes $1/\beta$ and $1/\gamma$, respectively. As seen in Fig.2(f), the linear fit yieldsthe$\beta$of 0.240 ± 0.006 with $T_C$of 67.91 ± 0.07 and $\gamma$of 1.000 ± 0.005 with $T_C$of 67.88 ± 0.05, respectively. Remarkably, the obtained values of the critical exponents and T_C using the KF method are in excellent agreement with those using the modified Arrott plot based on thetricritical mean-field model. This suggests that the estimated values are self-consistent and unambiguous.

To further validate the above critical exponents β andγ, we study the relation among these exponents. According to Eq. (S3), δ can be directly estimated from the critical isotherm at T_C. Figure 3 (a) shows the isothermal magnetization $M(H)$ at T_C = 67.9 K. The inset of the same plot has been demonstrated on a log−log scale. The solid straight line with a slope $1/\delta$ is the fitted result using Eq. (S3). From the linear fit we obtained the third critical exponent $\delta$of 5.032 ± 0.005.Moreover, the exponent δ can be calculated by the Widom scaling relation[49,50]

$$\delta = 1 + \gamma/\beta . \tag{3}$$

Based on the β and γ values calculated in Fig.2(e) and (f), Eq. (3)yields δof5.070 ± 0.006 and 5.167 ± 0.006, respectively. We emphasize that these values are very close to the results from the experimental critical isothermal analysis. Therefore, the critical exponents obtained in this study basically obey the Widom scaling relation, showing that the obtained β,$\gamma$and $\delta$are reliable.

Finally, these critical exponents should follow the scaling equation (Eq. (S6)) in

the critical region. The scaling equation indicates that *m* versus *h* forms two universal curves for $T>T_C$ and $T<T_C$, respectively. Based on Eq. (S7), the isothermal magnetization around the critical temperatures for $CrGeTe_3$ has been plotted in Fig.3 (b). All experimental data in the higher field region collapse onto two universal curves, in agreement with the scaling theory. The inset of Fig.3 (b) shows the corresponding log-log plot. Similarly, all the points also collapse into two different curves in the higher field region. This result shows again that the obtained results of the critical exponents and T_C are valid.

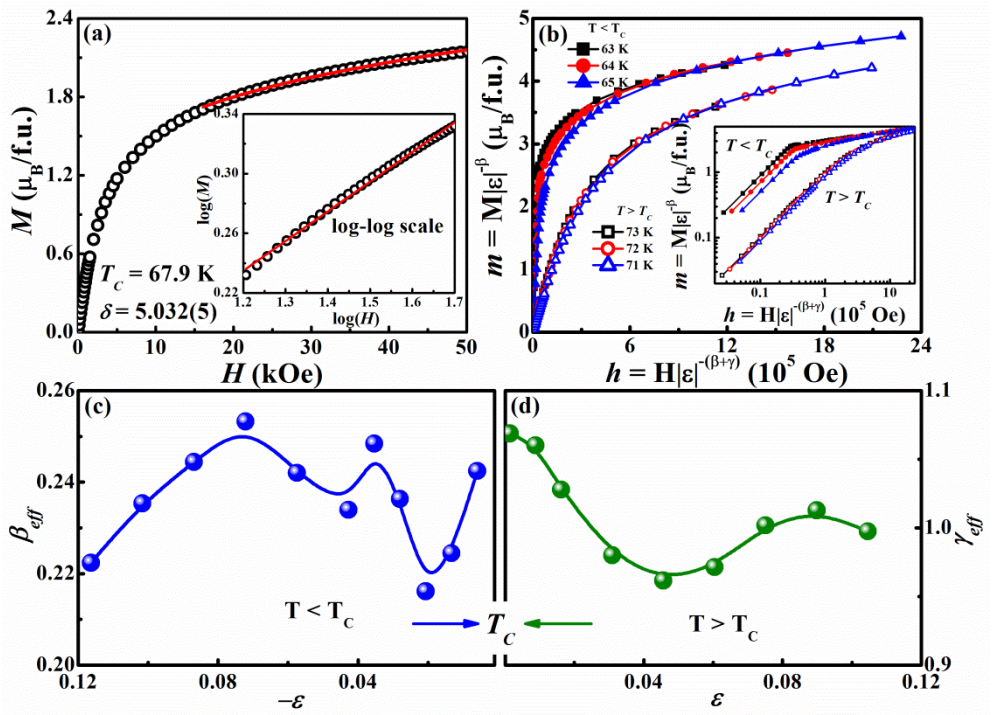

Figure 3.(Color online): (a) Isothermal $M(H)$ at T_C. The inset shows the alternative plot on a log-log scale and the straight line is the linear fit following Eq. (7); (b) Renormalized magnetization *m* versus renormalized field *h* at several typical temperatures around the T_C. The inset shows the alternative plot on a log-log scale; the effective exponents (c) β_{eff} below T_C and (d) γ_{eff} above T_C as a function of the reduced temperature ε.

To further examine the convergence of the critical exponents, the effective exponents β_{eff} and γ_{eff} can be are obtained by Eq. (S8) and (S9) for $CrGeTe_3$. As shown

in Fig.3 (c) and (d), both β_{eff} and γ_{eff} show a non-monotonic variation with ε (see Eq. (S4)). The lowest ε (ε_{min}) are 5.89×10^{-3} and 1.47×10^{-3} for β_{eff} and γ_{eff}, respectively. We obtain the effective exponents β_{eff} of 0.242 and γ_{eff} of1.069, indicating that both β_{eff} and γ_{eff} are converged when the temperature approaches T_C.

The experimentalcritical exponents of $CrGeTe_3$, as well as the theoretical values of $CrSiTe_3$, MnSi and some other manganitesbased on various models, are summarized in Table 1. It is seen that the critical exponents for MnSi and doped manganites are consistent with those of tricritical mean-field theory[46,47,51,52]. These compounds have the same characteristics, *i.e.*, a tricritical pointseparatingthe first-order from the second-order ferromagnetic phase transitions. This phenomenon shows that the element substitution[47,52], hole or electric doping[51], and external magnetic field[46] can induce the tricritical behavior. However, Cr*X*Te_3 presents a second-order ferromagnetic phase transitions[7,25-28] and our results indicate that the critical behavior of $CrGeTe_3$ is close to the theoretical value of tricritical mean-field model. Comparing with $CrSiTe_3$, showing characteristic of 2D-Ising model[7,34,35], the smaller van der Waals gap and the larger planar nearest-neighbor Cr-Cr distance of $CrGeTe_3$enhances the Curie temperature from 32K for the $CrSiTe_3$ to 61K for the $CrGeTe_3$[7,25-28]. In addition, the neutron scattering and isothermal magnetization experiments yield a critical exponent β of around 0.151 or 0.17 for $CrSiTe_3$[7,34,35], which is close to the value expected for a 2D transition ($\beta_{2D}^{\text{Ising}} = 0.125$) and well below the values expected for a3D transition ($\beta_{3D}^{\text{Ising}} = 0.326$).Our results yield a critical exponent β of 0.24 for $CrGeTe_3$ that is close to the critical exponent of the tricritical

mean-field model. Hence, the increase of the *X* atom radius, facilitating super exchange coupling between the Cr atoms via the Te atom andleading to the smaller van der Waals gap in Cr*X*Te_3 system [7,25-28], could induce a tricriticalmagnetic phase transition in the $CrGeTe_3$ single crystal.

Table 1. Critical exponents of $CrGeTe_3$ with various theoretical models, $CrSiTe_3$ and other related materials with tricritical mean-field model (SC = single crystal; PC = polycrystalline; cal = Calculated from Eq. (3)).

Composition	Reference	T_C (K)	Technique	β	γ	δ
$CrGeTe_3^{SC}$	This work	67.9	Modified Arrott plot	0.242 ± 0.006	0.985 ± 0.003	5.070 ± 0.006^{cal}
			Kouvel-Fisher method	0.240 ± 0.006	1.000 ± 0.005	5.167 ± 0.006^{cal}
			Criticalisotherm	-	-	5.032 ± 0.005
Tricritical mean-field	[45]	-	Theory	0.25	1	5
Mean-field	[43,44]	-	Theory	0.5	1	3
3D-Heisenberg theory	[43,44]	-	Theory	0.365	1.386	4.8
3D-Ising	[43,44]	-	Theory	0.325	1.24	4.82
$CrSiTe_3^{SC}$	[34]	31	Modified Arrott plot	0.170 ± 0.008	1.532 ± 0.001	10.012 ± 0.047^{cal}
$MnSi^{SC}$	[46]	30.5	Modified Arrott plot	0.242 ± 0.006	0.915 ± 0.003	4.734 ± 0.006
$La_{0.1}Nd_{0.6}Sr_{0.3}MnO_3^{PC}$	[47]	249.3	Modified Arrott plot	0.257 ± 0.005	1.12 ± 0.03	5.17 ± 0.02
$La_{0.9}Te_{0.1}MnO_3^{PC}$	[51]	239.5	Modified Arrott plot	0.201 ± 0.003	1.27 ± 0.04	7.14 ± 0.04
$La_{0.6}Ca_{0.4}MnO_3^{PC}$	[52]	265.5	Modified Arrott plot	0.25 ± 0.03	1.03 ± 0.05	5.0 ± 0.8

Although single-crystalline$CrSnTe_3$ has not yet been synthesized, we speculate that the magnetism of $CrSnTe_3$ should be closer to the 3D-Ising model. To support this assumption, we perform DFT calculations with the same calculation parameters that were used in Ref. [53]. Figure 4 (a) shows the calculated formation energyE_f, which is defined as the energy cost of extracting a sheet of single-layer CrXTe$_3$ from their bulk counterparts.As can be seen, E_f increases as the species vary from Si to Ge. This is consistent with the larger theoretical cleavage energy of single-layer $CrGeTe_3$than that of $CrSiTe_3$, which indicates that the layers are coupled more strongly in $CrGeTe_3$[31]. The formation energy of $CrSnTe_3$ is even higher than the other two compounds,revealing that it presentsthe strongest interlayer coupling, which leads to its 3D characteristics.Figure 4 (b), (c), and (d) illustrate the charge density of the three compounds. Consistent with the trend of the $E_f$results, the electron density around the Sn-Sn pairis the least amongthe three materials. Namely, more electrons in $CrSnTe_3$participate the interlayer coupling.

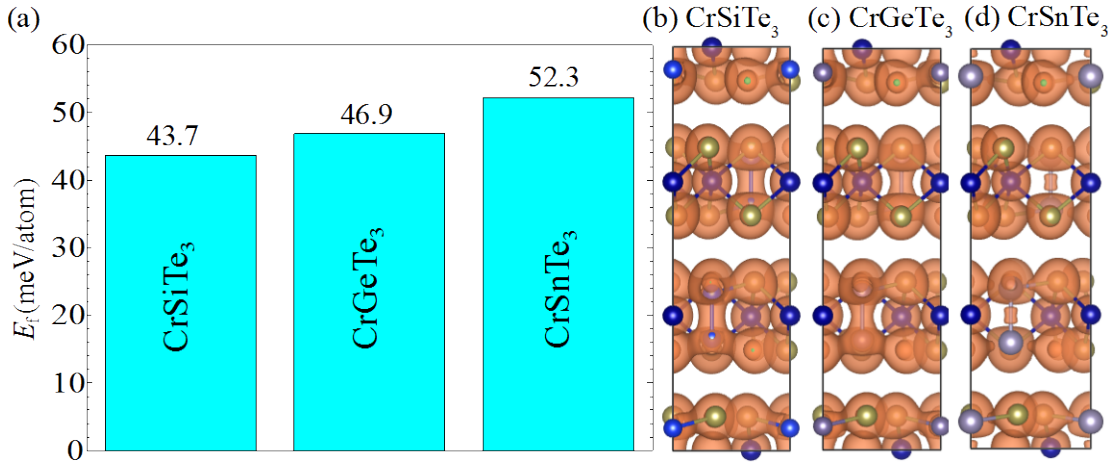

Figure 4. (Color online): (a) Formation energy of single-layer Cr*X*Te$_3$; The formation energy of single-layer CrSiTe$_3$ is adopted from Ref.[53](b), (c), and (d) Charge density of bulk Cr*X*Te$_3$with an isosurface value of 0.05 $e/r_{\mathrm{Bohr}}{}^3$.

In conclusion, we have performed a comprehensive experimental study on the critical properties of single-crystalline CrGeTe$_3$ using isothermal magnetization around the Curie temperatureT_C. Based on various experimental techniques including the modified Arrott plot, Kouvel-Fisher method and critical isotherm analysis, we obtained the critical exponents β, γ, and δ of 0.240 ± 0.006, 1.000 ± 0.005, and 5.070 ± 0.006, respectively, at the Curie temperature of 67.9 K.These numerical results are similar to the theoretical values in the tricritical mean-field model, which is therefore capable of describing the critical magnetic behavior of 2D CrGeTe$_3$.DFT calculations show that the formation energy of CrGeTe$_3$ lies between those of CrSiTe$_3$ and CrSnTe$_3$, which isin line with a crossover of the magnetic phase transition from 2D to 3D. Overall, our findings provide a fundamental understanding of the anomalous PM-FM transition in a novel 2D ferromagnetic semiconductor.

Acknowledgements

This work was supported by the National Key Research and Development Program under contracts 2016YFA0401803 and 2016YFA0300404, the Joint Funds of the

National Natural Science Foundation of China and the Chinese Academy of Sciences' Large-Scale Scientific Facility under contract U1432139and U1532153,the National Natural Science Foundation of China under contract11674326, Key Research Program of Frontier Sciences, CAS (QYZDB-SSW-SLH015), and the Nature Science Foundation of Anhui Province under contract 1508085ME103.J. Z. is supported by the Nature Science Foundation of China (Grant No. 51602079) and the Fundamental Research Funds for the Central Universities of China (Grant No. 372 AUGA5710013115). This research also used computational resources of the National Supercomputing Center of China in Shenzhen (Shenzhen Cloud Computing Center).

References

[1] K. S. Novoselov, A. K. Geim, S. V. Morozov, D. Jiang, Y. Zhang, S. V. Dubonos, I. V. Grigorieva, and A. A. Firsov, Science **306**, 666 (2004).
[2] K. S. Novoselov, A. K. Geim, S. V. Morozov, D. Jiang, M. I. Katsnelson, I. V. Grigorieva, S. V. Dubonos, and A. A. Firsov, Nature **438**, 197 (2005).
[3] Y. Zhang, Y.-W. Tan, H. L. Stormer, and P. Kim, Nature **438**, 201 (2005).
[4] A. K. Geim and K. S. Novoselov, Nat. Mater.**6**, 183 (2007).
[5] A. H. Castro Neto, F. Guinea, N. M. R. Peres, K. S. Novoselov, and A. K. Geim, Rev. Mod. Phys. **81**, 109 (2009).
[6] N. Zibouche, A. Kuc, J. Musfeldt, and T. Heine, Ann. Phys. (Berlin) **526**, 395 (2014).
[7] T. J. Williams, A. A. Aczel, M. D. Lumsden, S. E. Nagler, M. B. Stone, J. Q. Yan, and D. Mandrus, Phys. Rev. B **92**, 144404 (2015).
[8] I. Žutić, J. Fabian, and S. Das Sarma, Rev. Mod. Phys. **76**, 323 (2004).
[9] A. H. MacDonald, P. Schiffer, and N. Samarth, Nat. Mater. **4**, 195 (2005).
[10] T. Dietl, Nat. Mater. **9**, 965 (2010).
[11] Z. Deng, C. Q. Jin, Q. Q. Liu, X. C. Wang, J. L. Zhu, S. M. Feng, L. C. Chen, R. C. Yu, C. Arguello, T. Goko, F. Ning, J. Zhang, Y. Wang, A. A. Aczel, T. Munsie, T. J. Williams, G. M. Luke, T. Kakeshita, S. Uchida, W. Higemoto, T. U. Ito, B. Gu, S. Maekawa, G. D. Morris, and Y. J. Uemura, Nat. Commun. **2**, 422 (2011).
[12] Z. Y. Zhu, Y. C. Cheng, and U. Schwingenschlögl, Phys. Rev. B **84**, 153402 (2011).
[13] D. Xiao, G.-B. Liu, W. Feng, X. Xu, and W. Yao, Phys. Rev. Lett. **108**, 196802 (2012).
[14] W. Feng, Y. Yao, W. Zhu, J. Zhou, W. Yao, and D. Xiao, Phys. Rev. B **86**, 165108 (2012).
[15] W.-Y. Shan, H.-Z. Lu, and D. Xiao, Phys. Rev. B **88**, 125301 (2013).

[16] X. Xu, W. Yao, D. Xiao, and T. F. Heinz, Nat. Phys. **10**, 343 (2014).
[17] W. Han, R. K. Kawakami, M. Gmitra, and J. Fabian, Nat. Nano. **9**, 794 (2014).
[18] H. Ohno, D. Chiba, F. Matsukura, T. Omiya, E. Abe, T. Dietl, Y. Ohno, and K. Ohtani, Nature **408**, 944 (2000).
[19] C.-Z. Chang, J. Zhang, X. Feng, J. Shen, Z. Zhang, M. Guo, K. Li, Y. Ou, P. Wei, L.-L. Wang, Z.-Q. Ji, Y. Feng, S. Ji, X. Chen, J. Jia, X. Dai, Z. Fang, S.-C. Zhang, K. He, Y. Wang, L. Lu, X.-C. Ma, and Q.-K. Xue, Science **340**, 167 (2013).
[20] X. Kou, S.-T. Guo, Y. Fan, L. Pan, M. Lang, Y. Jiang, Q. Shao, T. Nie, K. Murata, J. Tang, Y. Wang, L. He, T.-K. Lee, W.-L. Lee, and K. L. Wang, Phys. Rev. Lett. **113**, 137201 (2014).
[21] Z. Wang, C. Tang, R. Sachs, Y. Barlas, and J. Shi, Phys. Rev. Lett. **114**, 016603 (2015).
[22] H. González-Herrero, J. M. Gómez-Rodríguez, P. Mallet, M. Moaied, J. J. Palacios, C. Salgado, M. M. Ugeda, J.-Y. Veuillen, F. Yndurain, and I. Brihuega, Science **352**, 437 (2016).
[23] C. Gong, L. Li, Z. Li, H. Ji, A. Stern, Y. Xia, T. Cao, W. Bao, C. Wang, and Y. Wang, Nature (2017).
[24] N. Sivadas, M. W. Daniels, R. H. Swendsen, S. Okamoto, and D. Xiao, Phys. Rev. B **91**, 235425 (2015).
[25] V. Carteaux, D. Brunet, G. Ouvrard, and G. Andre, J. Phys.: Condens. Matter **7**, 69 (1995).
[26] H. Ji, R. A. Stokes, L. D. Alegria, E. C. Blomberg, M. A. Tanatar, A. Reijnders, L. M. Schoop, T. Liang, R. Prozorov, K. S. Burch, N. P. Ong, J. R. Petta, and R. J. Cava, J. Appl. Phys. **114**, 114907 (2013).
[27] Y. Tian, M. J. Gray, H. Ji, R. Cava, and K. S. Burch, 2D Materials **3**, 025035 (2016).
[28] H. L. Zhuang, Y. Xie, P. R. C. Kent, and P. Ganesh, Phys. Rev. B **92**, 035407 (2015).
[29] B. Siberchicot, S. Jobic, V. Carteaux, P. Gressier, and G. Ouvrard, J. Phys. Chem. **100**, 5863 (1996).
[30] S. Lebègue, T. Björkman, M. Klintenberg, R. M. Nieminen, and O. Eriksson, Phys. Rev. X **3**, 031002 (2013).
[31] X. Li and J. Yang, J. Mater. Chem. C **2**, 7071 (2014).
[32] J. Zhang, B. Zhao, Y. Yao, and Z. Yang, Phys. Rev. B **92**, 165418 (2015).
[33] J. Liu, S. Y. Park, K. F. Garrity, and D. Vanderbilt, Phys. Rev. Lett. **117**, 257201 (2016).
[34] B. Liu, Y. Zou, L. Zhang, S. Zhou, Z. Wang, W. Wang, Z. Qu, and Y. Zhang, Sci. Rep. **6**, 33873 (2016).
[35] V. Carteaux, F. Moussa, and M. Spiesser, EPL Europhys. Lett. **29**, 251 (1995).
[36] G. Kresse and J. Furthmüller, Phys. Rev. B **54**, 11169 (1996).
[37] D. M. Ceperley and B. J. Alder, Phys. Rev. Lett. **45**, 566 (1980).
[38] J. P. Perdew and A. Zunger, Phys. Rev. B **23**, 5048 (1981).
[39] P. E. Blöchl, Phys. Rev. B **50**, 17953 (1994).
[40] G. Kresse and D. Joubert, Phys. Rev. B **59**, 1758 (1999).

[41] C. Kittel, *Introduction to Solid State Physics*. (Wiley, 2004).
[42] A. Arrott, Phys. Rev. **108**, 1394 (1957).
[43] S. N. Kaul, J. Magn. Magn. Mater. **53**, 5 (1985).
[44] N. Khan, P. Mandal, K. Mydeen, and D. Prabhakaran, Phys. Rev. B **85**, 214419 (2012).
[45] B. K. Banerjee, Phys. Lett. **12**, 16 (1964).
[46] L. Zhang, D. Menzel, C. Jin, H. Du, M. Ge, C. Zhang, L. Pi, M. Tian, and Y. Zhang, Phys. Rev. B **91**, 024403 (2015).
[47] J. Fan, L. Ling, B. Hong, L. Zhang, L. Pi, and Y. Zhang, Phys. Rev. B **81**, 144426 (2010).
[48] J. S. Kouvel and M. E. Fisher, Phys. Rev. **136**, A1626 (1964).
[49] B. Widom, J. Chem. Phys. **43**, 3898 (1965).
[50] B. Widom, J. Chem. Phys. **41**, 1633 (1964).
[51] J. Yang, Y. Lee, and Y. Li, Phys. Rev. B **76**, 054442 (2007).
[52] D. Kim, B. Revaz, B. L. Zink, F. Hellman, J. J. Rhyne, and J. F. Mitchell, Phys. Rev. Lett. **89**, 227202 (2002).
[53] M.-W. Lin, H. L. Zhuang, J. Yan, T. Z. Ward, A. A. Puretzky, C. M. Rouleau, Z. Gai, L. Liang, V. Meunier, B. G. Sumpter, P. Ganesh, P. R. C. Kent, D. B. Geohegan, D. G. Mandrus, and K. Xiao, J. Mater. Chem. C **4**, 315 (2016).